Simulating Oil Droplet Dispersal From the *Deepwater Horizon* Spill With a Lagrangian Approach

Elizabeth W. North,[1] E. Eric Adams,[2] Zachary Schlag,[1] Christopher R. Sherwood,[3] Ruoying He,[4] Kyung Hoon Hyun,[4] and Scott A. Socolofsky[5]

An analytical multiphase plume model, combined with time-varying flow and hydrographic fields generated by the 3-D South Atlantic Bight and Gulf of Mexico model (SABGOM) hydrodynamic model, were used as input to a Lagrangian transport model (LTRANS), to simulate transport of oil droplets dispersed at depth from the recent *Deepwater Horizon* MC 252 oil spill. The plume model predicts a stratification-dominated near field, in which small oil droplets detrain from the central plume containing faster rising large oil droplets and gas bubbles and become trapped by density stratification. Simulated intrusion (trap) heights of ~ 310–370 m agree well with the midrange of conductivity-temperature-depth observations, though the simulated variation in trap height was lower than observed, presumably in part due to unresolved variability in source composition (percentage oil versus gas) and location (multiple leaks during first half of spill). Simulated droplet trajectories by the SABGOM-LTRANS modeling system showed that droplets with diameters between 10 and 50 μm formed a distinct subsurface plume, which was transported horizontally and remained in the subsurface for >1 month. In contrast, droplets with diameters ≥90 μm rose rapidly to the surface. Simulated trajectories of droplets ≤50 μm in diameter were found to be consistent with field observations of a southwest-tending subsurface plume in late June 2010 reported by *Camilli et al.* [2010]. Model results suggest that the subsurface plume looped around to the east, with potential subsurface oil transport to the northeast and southeast. Ongoing work is focusing on adding degradation processes to the model to constrain droplet dispersal.

[1]University of Maryland Center for Environmental Science, Horn Point Laboratory, Cambridge, Maryland, USA.

[2]Department of Civil and Environmental Engineering, Massachusetts Institute of Technology, Cambridge, Massachusetts, USA.

[3]U. S. Geological Survey, Coastal and Marine Geology, Woods Hole, Massachusetts, USA.

[4]Department of Marine, Earth and Atmospheric Sciences, North Carolina State University, Raleigh, North Carolina, USA.

[5]Zachry Department of Civil Engineering, Coastal and Ocean Engineering Division, Texas A&M University, College Station, Texas, USA.

Monitoring and Modeling the *Deepwater Horizon* Oil Spill:
A Record-Breaking Enterprise
Geophysical Monograph Series 195

10.1029/2011GM001102

1. INTRODUCTION

We simulate the subsurface dispersal of oil in the Gulf of Mexico resulting from the *Deepwater Horizon* (DH) MC 252 spill, with the objective of predicting the spread of different size classes of oil droplets over time. At distances greater than a few hundred meters above the deepwater source (depending on ambient current speed and stratification), the buoyant jet, which is formed by the momentum of the initial release and the buoyancies of the gas and oil, breaks down. The subsequent oil dispersal depends mainly on advection and dispersion by ocean currents and on the behavior of oil droplets, which are fractionated into different sizes [*Socolofsky and Adams*, 2002; *Adams and Socolofsky*, 2005]. These oil droplets can have orders of magnitude differences

in rise velocities (e.g., 6 and 0.06 mm s^{-1} for 300 and 30 μm diameter particles, respectively) and also change in diameter as they age. These rise velocities fundamentally control whether the droplets reach the surface, and if they form subsurface plumes, and determine the direction and extent of horizontal dispersal. In addition, the use of dispersants changes droplet sizes and can substantially decrease rise velocities which in turn will affect horizontal dispersal [*NRC*, 2005].

The objective of our program is to investigate the far-field subsurface and surface dispersal of different size classes of oil released from the DH well. The research presented in this paper includes: (1) a description of the coupled plume, hydrodynamic, and Lagrangian model system applied in this effort, (2) comparison of model predictions with observations of a subsurface plume location [*Camilli et al.*, 2010], and (3) results of simulations that examine the sensitivity of far-field oil transport on the diameter of oil droplets.

2. METHODS

This section includes a description of the coupled plume, hydrodynamic, and Lagrangian model system as well as the model simulations that were conducted.

2.1. Model Description

2.1.1. Plume model. While more comprehensive integral plume models exist [e.g., *Zheng et al.*, 2003; *Johansen*, 2003], we chose to model the behavior of the near-field plume with a set of empirical algebraic equations describing characteristics of multiphase plumes. Multiphase plumes differ from single-phase plumes (e.g., wastewater discharged into seawater) in that the gas bubbles and larger oil droplets that are the source of buoyancy can separate from the entrained seawater plume as it becomes trapped by stratification or deflected by ambient currents. Empirical relationships characterizing multiphase plumes have been developed from laboratory experiments with air bubbles, glass beads (creating inverted, downward falling plumes), crude oil, and buoyant continuous-phase tracers in stratified and flowing conditions [*Akar and Jirka*, 1995; *Socolofsky and Adams*, 2002, 2003, 2005]. The experiments indicate that plume characteristics are governed by five parameters: horizontal velocity U; ambient density gradient, given by the buoyancy frequency $N = [(-g/\rho_r)(d\rho_a/dz)]^{1/2}$; gas bubble slip velocity u_s; source buoyancy flux $B_o = Q_o(\rho_a - \rho_o)/\rho_r$; and height z above the discharge, where g is gravitational acceleration, ρ_r and $\rho_a(z)$ are reference and ambient seawater potential densities, and ρ_o and Q_o are the potential density and volume flow rate of the initial oil/gas mixture.

The exact behavior depends on the relative importance of horizontal currents and stratification (Figures 1a to 1c), as discussed in the work *Socolofsky and Adams* [2002]. When horizontal currents dominate, the bubbles and large droplets exit at a separation height h_S, leaving a wake of entrained seawater with dissolved and finely dispersed hydrocarbons. When stratification dominates, the plume reaches a peel height h_P, where dispersed-phase buoyancy can no longer lift the entrained seawater; an outer downdraught plume of dissolved and finely dispersed hydrocarbons and seawater is created that eventually traps, forming a horizontal intrusion at a level of neutral buoyancy, h_T. Laboratory experiments suggest that the plume is dominated by horizontal currents if $h_S < h_P$ and by stratification if $h_s > h_p$. Our recent analysis [*Socolofsky et al.*, 2011] suggests that the DH plume was generally stratification dominated, and hence the main effect of the ambient currents was to carry the intrusions downstream.

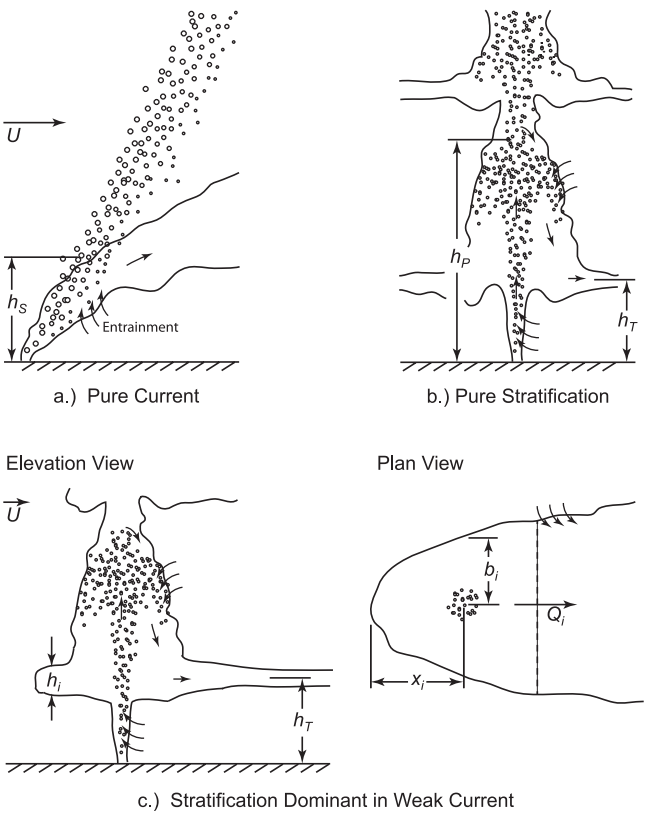

Figure 1. Schematic behavior of oil well blowout for (a) pure current and (b) pure stratification, and (c) stratification dominated plumes in weak current. Circles and dots represent gas bubbles and large oil droplets, and curved lines indicate edge of the plume containing small droplets, dissolved hydrocarbons, and entrained seawater. From the work of *Socolofsky et al.* [2011].

The trap height of a stratification-dominated plume is given by:

$$h_T/(B_o/N^3)^{1/4} = 2.9\exp[-(u_s/(B_oN)^{1/4}-1.0)^2/27.0] \quad (1)$$

Trap height decreases with ambient stratification, increases mildly with plume buoyancy, and (for moderate rise velocities) shows weak dependence on bubble/droplet size. Additional plume characteristics, including intrusion flow rate, size, and shape are provided in the work of *Socolofsky et al.* [2011].

Some judgment was necessary in model schematization and parameter selection. Buoyancy is contributed by both oil and gas, so the value of B_o was based on $B_{o,\mathrm{oil}} + B_{o,\mathrm{gas}}$. Fixed relative proportions of gas and oil were obtained from the work of *Lehr et al.* [2010]. It is known that some of the natural gas was dissolved in oil, and some reacted with water to form solid hydrate particles. Both processes would result in reduced buoyancy. Buoyancy would also vary with gas expansion and dissolution into water, but because of uncertainty regarding the magnitudes of these processes, it was assumed that all of the natural gas was in the form of pure gas bubbles with constant mass and volume. Prior to 3 June 2010, there were two leaks, separated by several hundred meters. While these likely formed separate, noninteracting plumes, they were treated as a single source. The slip velocity u_s describes the motion of the dispersed phase relative to the continuous phase and predicts the tendency for phase separation. Because of their larger size and lower density, gas bubbles rise faster than oil bubbles. Bubbles with sizes of 5 to 20 mm have similar slip velocities (~20 cm s^{-1}), while 1 mm bubbles have a slip velocity of 10 cm s^{-1}, and 0.5 mm bubbles have a slip velocity of 4 cm s^{-1} [*Clift et al.*, 1978]. Trap heights are insensitive to rise velocity in this range, and we used a value of u_s = 0.21 m s^{-1}, which matches the velocity of 20 mm bubbles. Finally, vertical profiles of potential density were obtained from conductivity-temperature-depth casts taken near the wellhead. These profiles indicate that potential density varied quadratically with elevation, so equation (1) was recast for a quadratic fit to potential density (linear N) rather than a linear fit (constant N); details are provided in the work of *Socolofsky et al.* [2011]. The resulting model provided an estimate of the time-varying trap height (Figure 2), which was used to initialize the Lagrangian simulation of oil droplets described below. Figure 2 also includes model

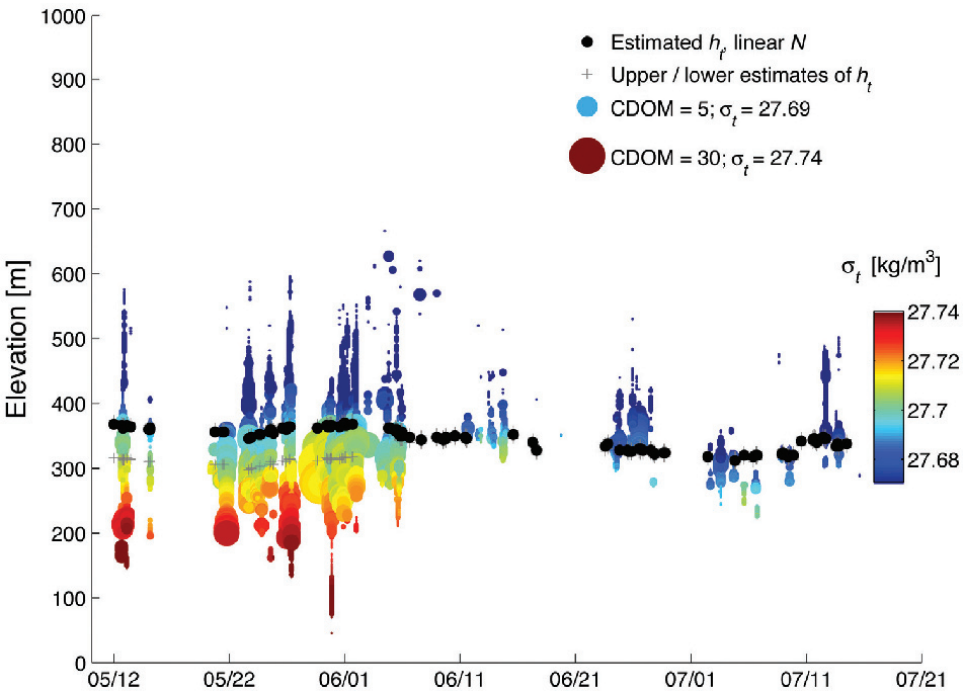

Figure 2. Time-series comparison of fluorescence measurements (colored dots) with predicted trap height h_T (black dots; upper and lower estimates shown with gray crosses). Size of the colored dots represents the amount of "excess" fluorescence; color of the dots indicates potential density as σ_t (ρ − 1000 kg m^{-3}). From the work of *Socolofsky et al.* [2011].

sensitivity results which are described further in the work of *Socolofsky et al.* [2011].

2.1.2. Hydrodynamic model. Circulation patterns and hydrography in the Gulf of Mexico during the DH spill were simulated with the South Atlantic Bight and Gulf of Mexico model (SABGOM). The model is based on the Regional Ocean Modeling System (ROMS) and has 5 km horizontal resolution and 36 vertical layers. It is nested inside the data assimilative global HYbrid Coordinate Ocean Model (1/12° resolution) [cf. *Chassignet et al.*, 2009]. Realistic tidal and meteorological forcing and runoff of major rivers in the region are included in the SABGOM model simulations. Details of model configuration have been reported by *Hyun and He* [2010]. During the DH oil spill event, the output of SABGOM forecasts was incorporated in the multiple-model surface trajectory forecast by researchers at University of South Florida [*Liu et al.*, this volume] and NOAA Emergency Response Division [*MacFadyen et al.*, this volume]. A hindcast was run with SABGOM to provide input to the Lagrangian model (described below). Hourly SABGOM output was stored to resolve changes in current velocities at tidal time scales. Output of the hydrodynamic model included 3-D fields of temperature, salinity, density, and diffusivities, three components of velocity, and sea surface height. An example of current velocities predicted by the SABGOM can be found in Figure 3.

2.1.3. Lagrangian model. The Lagrangian transport model (LTRANS) is adapted for this effort and uses the stored SABGOM predictions to calculate particle movement in 5 min time steps. LTRANS is an off-line particle-tracking

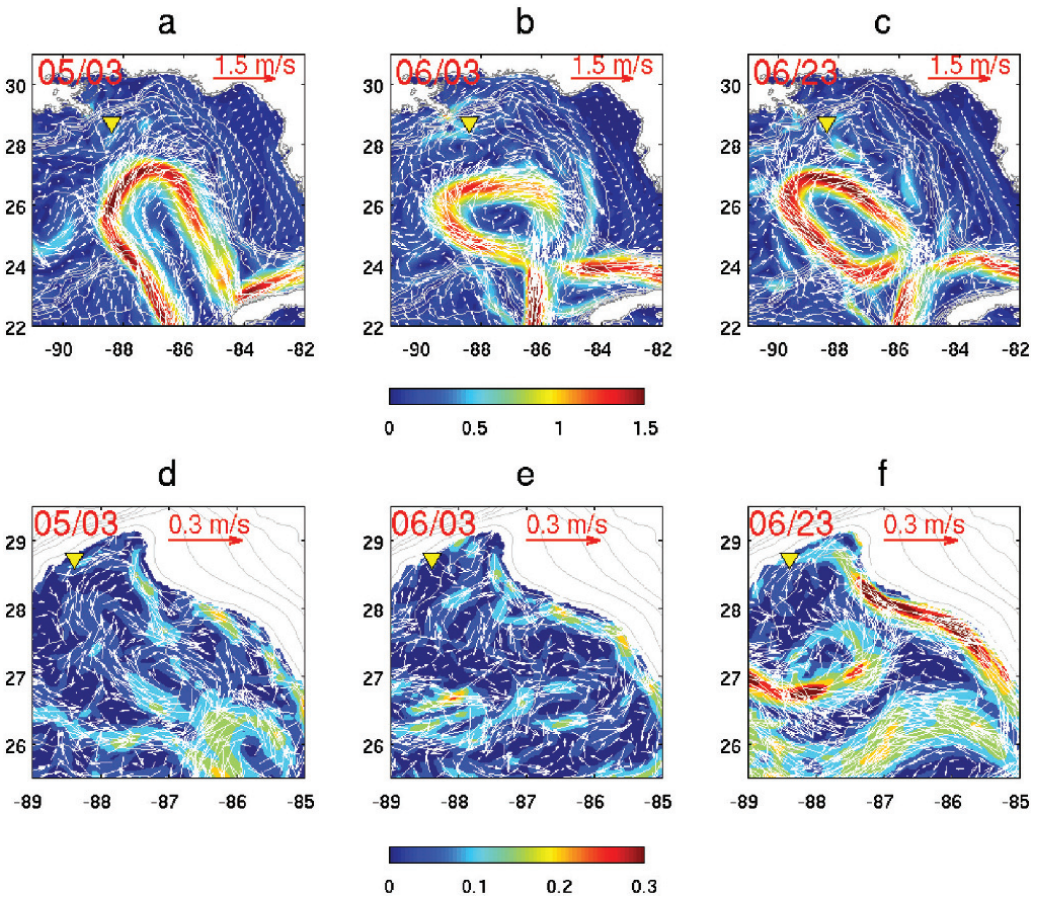

Figure 3. Current velocities at the surface (a, b, c) and at 1100 m (d, e, f) on 3 May (a, d), 3 June (b, e), and 23 June 2010 (c, f) predicted by the SABGOM ROMS model. Color contours indicate current velocity magnitude (m s^{-1}) and differ between upper and lower panels. White arrows are current velocity vectors. The date and velocity vector scale are in red at the top of each panel. The yellow triangle marks the location of the *Deepwater Horizon* well. The deep currents (bottom panels) are zoomed in to better resolve currents near the DH site.

model that runs with the stored predictions generated by ROMS models. It tracks the trajectories of particles in three dimensions using advection, mixing, and behavior such as oil droplet rise velocities or swimming behavior for biological particles [*North et al.*, 2006, 2008; *Schlag et al.*, 2008]. The off-line design was chosen to focus computational power on running sufficient number of particles to ensure statistical robustness of model results [*Brickman and Smith*, 2002; *Brickman et al.*, 2009]. It interpolates sea surface height, three components of velocities, salinity, temperature, and diffusivities from the native grid locations and includes a fourth-order Runge-Kutta scheme for particle advection. In addition, a random component is added to particle motion in order to simulate subgrid scale turbulent diffusion [*Hunter et al.*, 1993; *Visser*, 1997; *Brickman and Smith*, 2002] using a random displacement model [*Visser*, 1997]. Vertical boundary conditions are reflective if a particle passes through the surface or bottom boundary due to turbulence or vertical advection. If a particle passes through the surface due to behavior (e.g., oil droplet rise velocity), the particle is placed just below the surface (i.e., it stops near the boundary). Reflective horizontal boundary conditions are used to keep particles within the model domain, except at open ocean boundaries where particle movement is stopped.

Particles were assigned characteristics of oil droplets, including diameter, density, and rise velocity. The size distribution of nondispersed oil emanating from a blowout has been measured in the lab [*Masutani and Adams*, 2000], observed in the field [*Johansen*, 2003], and simulated theoretically [*Chen and Yapa*, 2007]. As an example, *Masutani and Adams* [2000] suggest that over 30% of the oil resulting from a high-energy ("atomizing mode") release may be composed of droplets with diameters of less than 0.5 mm. While there has been virtually no experience with the effectiveness of chemical dispersants applied at the source of a blowout, experiments with dispersants applied at the surface suggest that dispersant may decrease droplet size by one to two orders of magnitude [*NRC*, 2005]. With this background, droplet sizes in the range of 10 to 300 μm were simulated. Rise velocities were based on the work of *Zheng and Yapa* [2000]. Oil droplet density was fixed at 858 kg m^{-3} [*Socolofsky et al.*, 2011], and water density and dynamic viscosity were determined after interpolating SABGOM salinity and temperature to the particle location.

Tests were conducted with passive, neutrally buoyant particles to determine if numerical diffusion was present in the Lagrangian model. Numerical diffusion results in unintended, artificial dispersion of particles and can be especially confounding when rise velocities or advection velocities are small. In the first of two tests for numerical diffusion, vertical and horizontal current velocities were set to zero, and subgrid

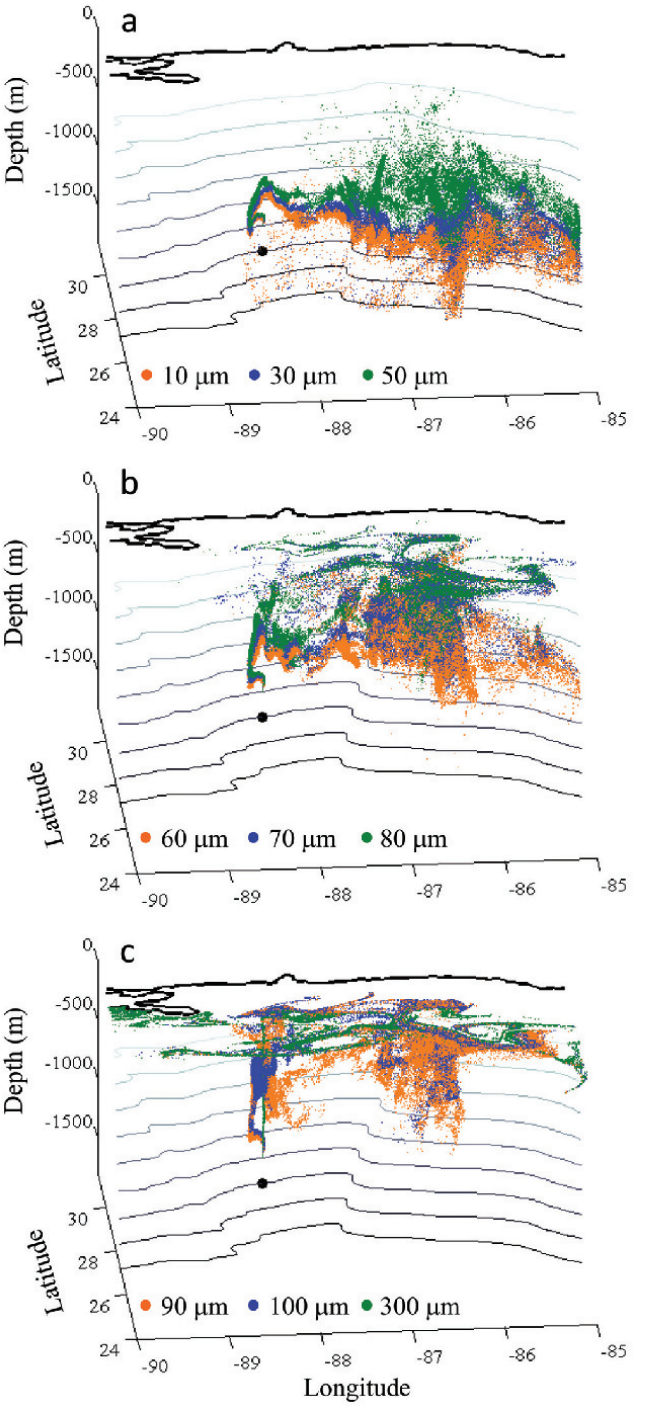

Figure 4. Snapshot of particle distributions on 3 June 2010 for different sizes of oil droplets: (a) 10, 30, and 50 μm, (b) 60, 70, and 80 μm, and (c) 90, 100, and 300 μm. Colors of particles represent diameter of oil droplets (key at bottom of each panel). Bottom depth contours are in 200 m intervals. The black circle indicates the location of the DH well. Particles were released at the time-varying trap height above this location.

scale turbulence was turned off. After 100 days, particles were in the same location in which they started. In the second test, particle rise velocities were set to zero, vertical current velocities were set to zero, and subgrid scale turbulence was turned off, so particles were moved only by horizontal advection. After 100 days, particles were at the same depth at which they started, except for those that intersected with the bathymetry. These tests indicate that numerical diffusion is not present in the Lagrangian model and that oil droplet transport is due to the intended physics in the model system.

2.2. Coupled Model Simulations

Model simulations were conducted with several fixed-diameter droplet sizes to examine the sensitivity of horizontal and vertical transport to oil droplet diameter. Particles were released in a continuous stream at the location of the DH spill (28.738°N, 88.366°W) beginning on 22 April 2010 and ending on 15 July 2010. The depth of particle release varied with trap height estimated by the plume model (Figure 2, black dots). The number of particles released per time step was proportional to the time-varying flow rate of oil from the well [*McNutt et al.*, 2011]. Nine simulations were conducted, each with a different initial diameter for the oil droplets, which did not change over the course of the model run (i.e., degradation processes were not included). The diameters were: 10, 30, 50, 60, 70, 80, 90, 100, and 300 μm. A total of 81,609 particles were tracked in each simulation.

Model results were examined to determine which size particles resulted in subsurface plumes. In addition, model results were compared to observations of the subsurface plume on 23–28 June 2010 described by *Camilli et al.* [2010] by plotting particle concentrations in relation to the transect on which the subsurface plume was observed [Figure 3A of *Camilli et al.*, 2010]. Finally, the distribution of particles that created subsurface plumes was plotted on 3 May, 3 June, and 3 July 2010 to examine the time evolution of the oil plume and the transport of droplets. Particle numbers were converted to oil concentrations using the known discharge rate of oil and the input droplet rates and sizes. For this purpose, droplets in the slow-rising size range of 10 to 50 μm were assumed to constitute 30% of the released oil, 10% each in a class of 10, 30 and 50 μm. This assumption is based on the conclusion by *Ryerson et al.* [2011] that up to two thirds of the oil was either captured or found on the surface within a relatively narrow radius of the source.

3. RESULTS

Model simulations with fixed-diameter particles indicate that oil droplet diameter significantly influenced the transport of oil from the DH spill. Predicted distributions on 3 July indicate that particles ≤50 μm formed subsurface plumes that remained below surface for >1 month (Figure 4a); particles with diameters between 60 and 80 μm rose slowly to the surface, dispersing through the water column (Figure 4b); particles with diameters of 90 and 100 μm rose rapidly to the surface with some subsurface dispersal (Figure 4c); particles with a diameter of 300 μm rose directly to the surface and remained there (Figure 4c). Note the transport of 300 μm particles to the west at the surface (Figure 4c), whereas subsurface particles looped around and were transported to the east (Figure 4a).

On 23–28 June 2010, *Camilli et al.* [2010] observed a southwest-tending subsurface plume between 1000 and 1200 m (their Figure 3A). Model simulations indicate that the plume extended to the east in early May, had a southwest bulge forming in early June, and showed a clear southwest-tending plume by 23 June (Figure 5, left panels). During the time of the *Camilli et al.* [2010] cruise (23–28 June), the predicted southwest-tending plume was aligned along the *Camilli et al.* transect. Particle depths were within the range of those observed by *Camilli et al.* or slightly above it (Figure 5, right panels). This qualitative agreement between model predictions and observations of the subsurface plume is quite good considering the simplified parameterizations of the plume, the single point location of oil release, and the lack of degradation processes associated with oil droplets.

The simulated distributions of 10, 30, and 50 μm droplets reproduce the subsurface plumes extending toward the southwest, as observed by *Camilli et al.* [2010]. However, particle distributions also suggest that subsurface oil was transported to the east and along the shelf/slope (Figure 6) by the predicted currents that tended in that direction (Figures 3d, 3f). Distinct subsurface plumes appear at 1000–1200 m on both 3 June and 3 July, whereas particle concentrations

Figure 5. (opposite) (left) Map view and (right) side view of subsurface particle distributions. Colors indicate particle diameter (red = 10 μm, blue = 30 μm, dark blue = 50 μm). Orange lines indicate the transect along which *Camilli et al*. [2010] reported evidence of a subsurface plume between 1000 and 1200 m. Date of model simulation is in upper left corner of each panel, ranging from (top) before the *Camilli et al*. [2010] observations (two rows) to (bottom) during the *Camilli et al.* cruises (two rows). Bottom depth contours are in 200 m intervals. The black circle in each panel indicates the location of the DH well. Particles were released at the time-varying trap height above this location (see black circle in Figure 4).

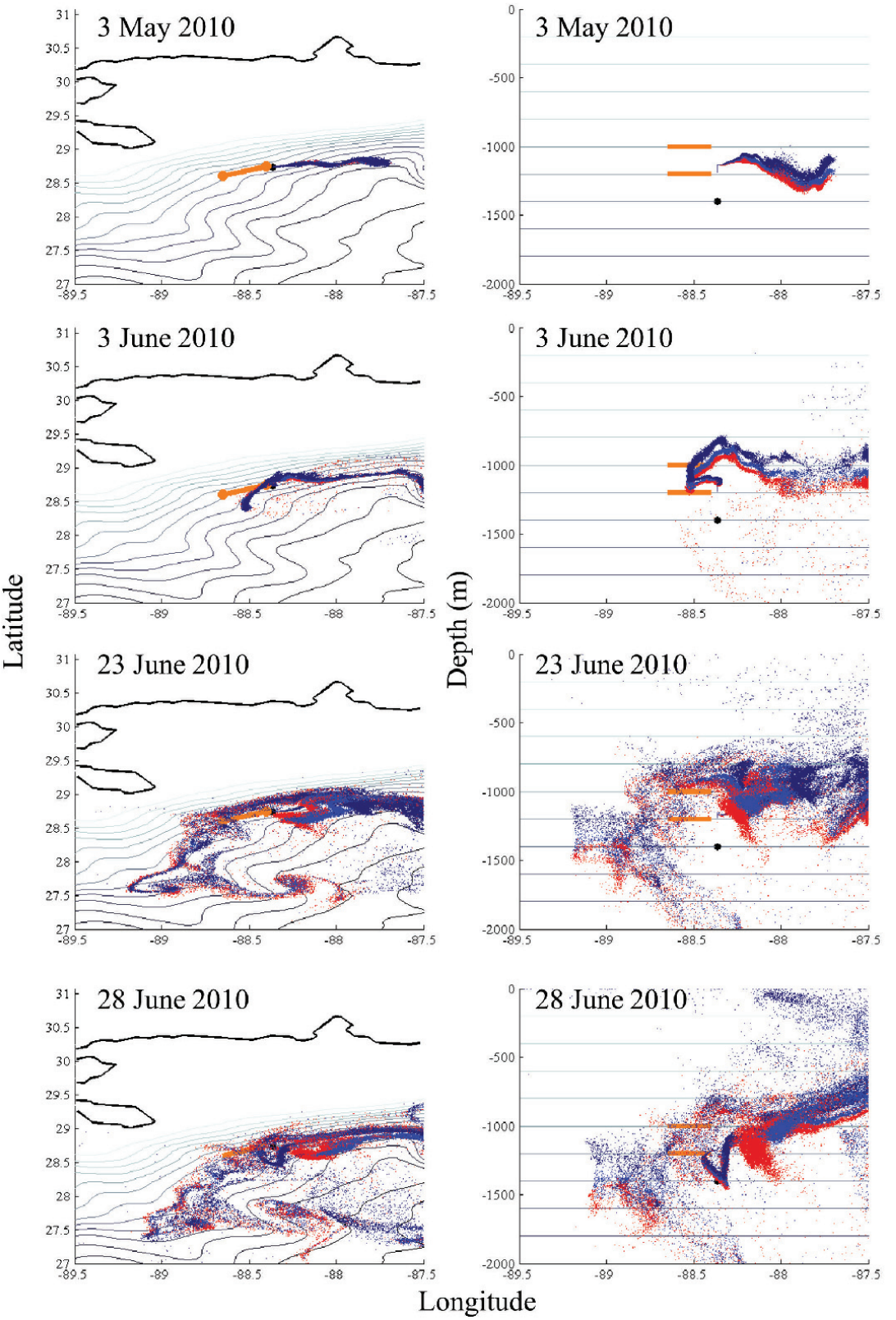
3 May 2010
3 May 2010
3 June 2010
3 June 2010
23 June 2010
23 June 2010
28 June 2010
28 June 2010
Latitude
Depth (m)
Longitude

Figure 5

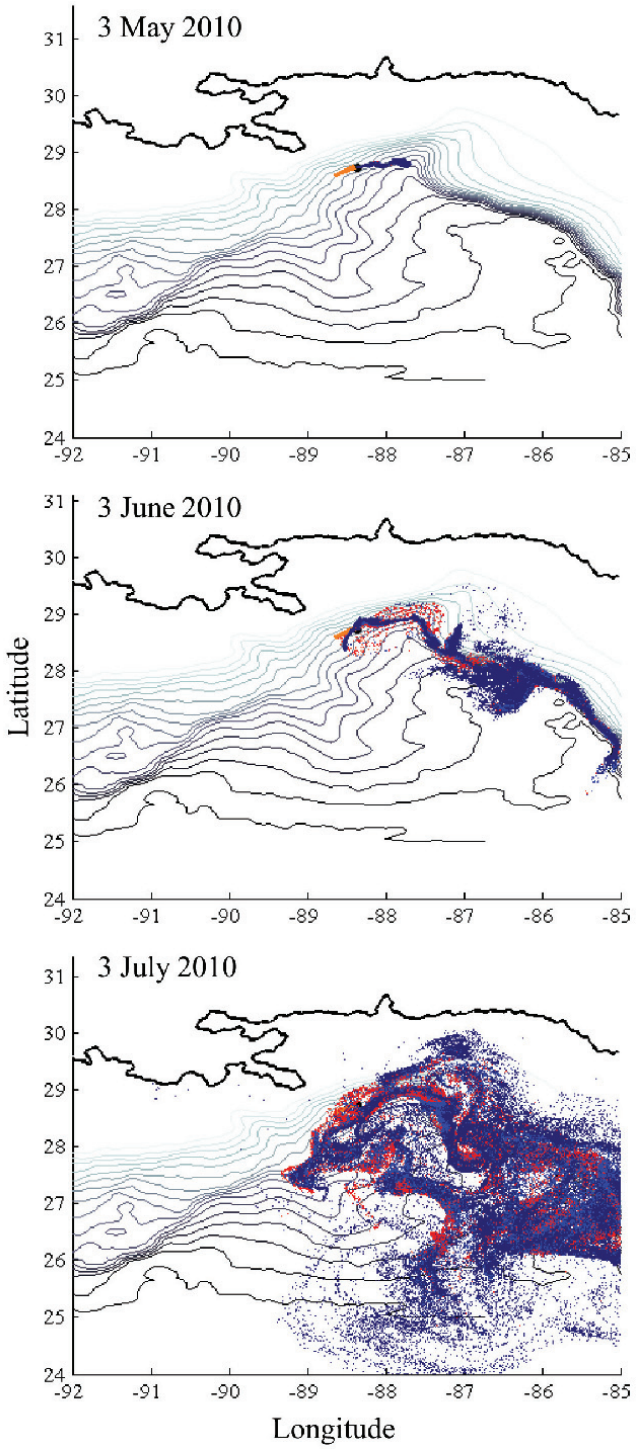

Figure 6. Map view of subsurface particle distributions on 3 May, 3 June, and 3 July 2010. Colors indicate particle diameter (red, 10 μm; blue, 30 μm; dark blue, 50 μm). Orange lines indicate the transect along which *Camilli et al*. [2010] reported evidence of a subsurface plume in between 1000 and 1200 m depth.

at mid-depth (400–600 m) and near-surface (0–200 m) on 3 July were more diffuse (Figure 7). Note that minor concentrations were predicted to be present in near-surface waters on 3 June, over a month after the DH spill had begun. Because degradation processes were not included in these simulations, these distributions can be regarded only as the maximum possible distribution of oil. Ongoing simulations with oil droplet degradation indicate that, although the transport patterns are similar, the extent of oil transport is highly sensitive to degradation processes and could have been less extensive than pictured here.

4. DISCUSSION

We present a coupled modeling system for simulating the transport of oil droplets dispersed at depth from the recent DH oil spill. An analytical multiphase plume model is used to provide the initial conditions for a LTRANS, which incorporates the output of a 3-D hydrodynamic model (SABGOM) to calculate the trajectory of oil droplets as they ascend and are advected and diffused over time. Numerical tests indicate that particle tracking calculations are not subject to numerical diffusion. Qualitative comparison with observations of the southwest-tending subsurface plume [*Camilli et al.*, 2010] showed good agreement. Model simulations indicate that droplet diameter significantly influenced oil droplet distributions and that oil may have been transported to the east in the subsurface in addition to the southwest. During the DH spill, sampling efforts were concentrated on the west side of the plume, so it is possible that a subsurface plume to the east could have been largely undetected.

The Lagrangian approach has advantages and disadvantages for simulating oil spills. The approach enables simulation of plumes that are smaller than the Eulerian model grid cells. It also can account for the interaction of time-varying droplet characteristics with time-varying physical conditions. Numerous model runs with varying particle characteristics and initial particle locations can be run without recomputing the hydrodynamics. In addition, numerical time steps can be longer, and numerical diffusion does not confound particle motion. The primary disadvantage is that the particle field cannot influence the hydrodynamics by, for example, changing the density or viscosity of seawater. In practice, this restricts the method to low concentrations. Another drawback is that many thousands of particles are required to adequately capture the probability distribution of particle transport. Computational resources can be demanding when running Lagrangian models with appropriate number of particles, although recent rapid increases in computational power diminish this concern.

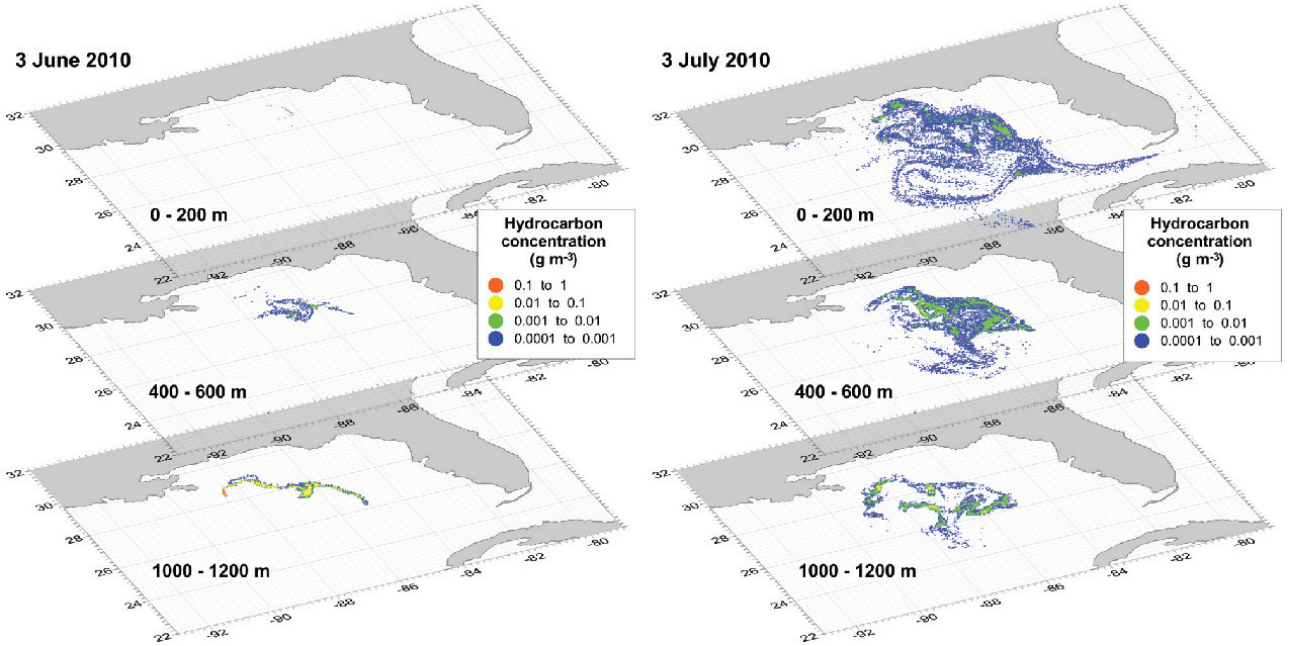

Figure 7. Estimated hydrocarbon concentrations on (left) 3 June 2010 and (right) 3 July 2010 at selected depths (0–200, 400–600, 1000–1200 m). Concentrations (kg m^{-3}) are the sum of the concentrations resulting from the distributions of 10, 30, and 50 μm diameter particles, assuming that 30% of the oil released from the DH spill went into these size classes.

Future oil-spill response models could use this approach to provide real-time forecasts of subsurface oil movement, and ongoing and planned improvements to this coupled model system will likely improve its predictive capabilities. Experimental and theoretical efforts by other investigators will be used to generate oil droplet size distributions with and without the presence of gas and chemical dispersants and predict transport. Instead of releasing particles at a fixed point, releases of clouds of particles corresponding to the dimensions of the trapped plume are ongoing. In addition, we are running sensitivity simulations with droplet degradation rates that correspond with observations by *Hazen et al.*, 2010 and others. Ongoing work is focusing on adding more realistic transformation processes to the droplet model (e.g., degrading droplet diameter and density) allowing the full potential of the Lagrangian approach to be realized.

Acknowledgments. We thank Richard Signell, CJ Beegle-Kraus, and Scott Peckham for helpful discussions and valuable information. The manuscript was improved following suggestions by R. Signell, Alfredo Aretxabaleta, and two anonymous reviewers. This research was funded by a National Science Foundation RAPID: *Deepwater Horizon* grant (OCE-1048630). The U.S. Geological Survey Coastal and Marine Geology Program supported C.R. Sherwood. This is UMCES-HPL contribution number 4571.

REFERENCES

Adams, E., and S. Socolofsky (2005), Review of deep oil spill modeling activity supported by the DeepSpill JIP and Offshore Operators Committee Bur. of Ocean Energy Manage., Washington, D. C. [Available at http://www.mms.gov/tarprojects/377.htm.]

Akar, P. J., and G. H. Jirka (1995), Buoyant spreading processes in pollutant transport andmixing Part 2: Upstream spreading in weak ambient current, *J. Hydraul. Res.*, *33*, 87–100.

Brickman, D., and P. C. Smith (2002), Lagrangian stochastic modeling in coastal oceanography, *J. Atmos. Ocean Technol.*, *19*, 83–99.

Brickman, D., B. Ådlandsvik, U. H. Thygesen, C. Parada, K. Rose, A. J. Hermann, and K. Edwards (2009), Particle tracking, *ICES Coop. Res. Rep. 295*, Int. Counc. for the Explor. of the Sea, Copenhagen V, Denmark.

Camilli, R., C. M. Reddy, D. R. Yoerger, B. A. S. Van Mooy, M. V. Jakuba, J. C. Kinsey, C. P. McIntyre, S. P. Sylva, and J. V. Maloney (2010), Tracking hydrocarbon plume transport and biodegradation at *Deepwater Horizon*, *Science*, *330*(6001), 201–204.

Chassignet, E. P., et al. (2009), U.S. GODAE: Global Ocean Prediction with the HYbrid Coordinate Ocean Model (HYCOM), *Oceanography*, *22*(2), 64–75.

Chen, F., and P. Yapa (2007), Estimating the oil droplet size distribution in deepwater oil spills, *J. Hydraul. Eng.*, *133*, 197–207.

Clift, R., J. Grace, and M. E. Weber (1978), *Bubbles, Drops and Particles*, Dover, New York.

Hazen, T. C., et al. (2010), Deep-sea oil plume enriches indigenous oil-degrading bacteria, *Science*, *330*, 204–208.

Hunter, J., P. Craig, and H. Phillips (1993), On the use of random-walk models with spatially-variable diffusivity, *J. Comput. Phys.*, *106*, 366–376.

Hyun, K. H., and R. He (2010), Coastal upwelling in the South Atlantic Bight: A revisit of the 2003 cold event using long term observations and model hindcast solutions, *J. Mar. Syst.*, *83*, 1–13.

Johansen, O. (2003), Development and verification of deep-water blowout models, *Mar. Pollut. Bull.*, *47*(9–12), 360–368.

Lehr, B., et al. (2010), Oil budget calculator—*Deepwater Horizon*, Fed. Interagency Solutions Group, Oil Budget Calculator Sci. and Eng. Team, Washington, D. C. [Available at http://www.crrc.unh.edu/publications/OilBudgetCalcReport_Nov2010.pdf, accessed February 1, 2011.]

Liu, Y., R. H. Weisberg, C. Hu, and L. Zheng (2011), Trajectory forecast as a rapid response to the *Deepwater Horizon* oil spill, in *Monitoring and Modeling the Deepwater Horizon Oil Spill: A Record-Breaking Enterprise*, *Geophys. Monogr. Ser.*, doi:10.1029/2011GM001121, this volume.

MacFadyen, A., G. Y. Watabayashi, C. H. Barker, and C. J. Beegle-Krause (2011), Tactical modeling of surface oil transport during the *Deepwater Horizon* spill response, in *Monitoring and Modeling the Deepwater Horizon Oil Spill: A Record-Breaking Enterprise*, *Geophys. Monogr. Ser.*, doi:10.1029/2011GM001128, this volume.

Masutani, S., and E. Adams (2000), Experimental study of multiphase plumes with application to deep ocean oil spills, final report, contract 1435-01-98-CT-30964, U.S. Dep. of the Inter., Miner. Manage. Serv., Herndon, Va., [Available at http://www.mms.gov/tarprojects/377.htm.]

McNutt, M., R. Camilli, G. Guthrie, P. Hsieh, V. Labson, B. Lehr, D. Maclay, A. Ratzel, and M. Sogge (2011), Assessment of flow rate estimates for the *Deepwater Horizon*/Macondo Well oil spill, in *Flow Rate Technical Group Report to the National Incident Command, Interagency Solutions Group, March 10, 2011*, U.S. Dep. of the Inter., Herndon, Va.

North, E. W., R. R. Hood, S. Y. Chao, and L. P. Sanford (2006), Using a random displacement model to simulate turbulent particle motion in a baroclinic frontal zone: A new implementation scheme and model performance tests, *J. Mar. Syst.*, *60*, 365–380.

North, E. W., Z. Schlag, R. R. Hood, M. Li, L. Zhong, T. Gross, and V. S. Kennedy (2008), Vertical swimming behavior influences the dispersal of simulated oyster larvae in a coupled particle-tracking and hydrodynamic model of Chesapeake Bay, *Mar. Ecol. Prog. Ser.*, *359*, 99–115.

NRC (2005), *Oil Spill Dispersants: Efficacy and Effects*, Natl. Res. Counc. of the Natl. Acad., The Natl. Acad. Press, Washington, D. C.

Ryerson, T. B., et al. (2011), Atmospheric emissions from the *Deepwater Horizon* spill constrain air-water partitioning, hydrocarbon fate, and leak rate, *Geophys. Res. Lett.*, *38*, L07803, doi:10.1029/2011GL046726.

Schlag, Z. R., E. W. North, and K. A. Smith (2008), *Larval TRANSport Lagrangian Model (LTRANS) Users Guide*, Univ. of Maryland Cent. for Environ. Sci., Horn Point Lab., Cambridge, Md.

Socolofsky, S. A., and E. E. Adams (2002), Multi-phase plumes in uniform and stratified crossflow, *J. Hydraul. Res.*, *40*(6), 661–672.

Socolofsky, S. A., and E. E. Adams (2003), Liquid volume fluxes in stratified multiphase plumes, *J. Hydraul. Eng.*, *129*(11), 905–914.

Socolofsky, S. A., and E. E. Adams (2005), Role of slip velocity in the behavior of stratified multiphase plumes, *J. Hydraul. Eng.*, *131*(4), 273–282.

Socolofsky, S. A., E. E. Adams, and C. R. Sherwood (2011), Formation dynamics of subsurface hydrocarbon intrusions following the *Deepwater Horizon* blowout, *Geophys. Res. Lett.*, *38*, L09602, doi:10.1029/2011GL047174.

Visser, A. W. (1997), Using random walk models to simulate the vertical distribution of particles in a turbulent water column, *Mar. Ecol. Prog. Ser.*, *158*, 275–281.

Zheng, L., and P. Yapa (2000), Buoyant velocity of spherical and nonspherical bubbles/droplets, *J. Hydraul. Eng.*, *126*, 852–854.

Zheng, L., P. Yapa, and F. H. Chen (2003), A model for simulating deepwater oil and gas blowouts—Part 1: Theory and model formulation, *J. Hydraul. Res.*, *41*(4), 339–351.

E. Adams, Department of Civil and Environmental Engineering, Massachusetts Institute of Technology, Rm 48-216b, Cambridge, MA 02139, USA.

R. He and K. H. Hyun, Department of Marine, Earth and Atmospheric Sciences, North Carolina State University, 2800 Faucette Drive, Raleigh, NC 27695-8208, USA.

E. W. North and Z. Schlag, University of Maryland Center for Environmental Science, Horn Point Laboratory, 2020 Horns Point Rd., Cambridge, MD 21613, USA. (enorth@umces.edu)

C. R. Sherwood, U. S. Geological Survey, Coastal and Marine Geology, 384 Woods Hole Rd., Woods Hole, MA 02543-1598, USA.

S. A. Socolofsky, Zachry Department of Civil Engineering, Coastal and Ocean Engineering Division, Texas A&M University, 3136 TAMU, College Station, TX 77843-3136, USA.